mathematics

MDPI

Article

Bifurcation Analysis and Solitons Dynamics of the Fractional Biswas–Arshed Equation via Analytical Method

Asim Zafar [1], Waseem Razzaq [1], Abdullah Nazir [1], Mohammed Ahmed Alomair [2], Abdulaziz S. Al Naim [3] and Abdulrahman Alomair [3,*]

[1] Department of Mathematics, COMSATS University Islamabad, Vehari Campus, Vehari 61100, Pakistan; asimzafar@cuivehari.edu.pk (A.Z.); mathcentr@gmail.com (W.R.); abdullahnazir0306@gmail.com (A.N.)
[2] Department of Quantitative Methods, School of Business, King Faisal University, Al-Ahsa 31982, Saudi Arabia; ma.alomair@kfu.edu.sa
[3] Department of Accounting, School of Business, King Faisal University, Al-Ahsa 31982, Saudi Arabia; asaudalnaim@kfu.edu.sa
* Correspondence: aamalomair@kfu.edu.sa

Abstract

This paper investigates soliton solutions of the time-fractional Biswas–Arshed (BA) equation using the Extended Simplest Equation Method (ESEM). The model is analyzed under two distinct fractional derivative operators: the β-derivative and the M-truncated derivative. These approaches yield diverse solution types, including kink, singular, and periodic-singular forms. Also, in this work, a nonlinear second-order differential equation is reconstructed as a planar dynamical system in order to study its bifurcation structure. The stability and nature of equilibrium points are established using a conserved Hamiltonian and phase space analysis. A bifurcation parameter that determines the change from center to saddle-type behaviors is identified in the study. The findings provide insight into the fundamental dynamics of nonlinear wave propagation by showing how changes in model parameters induce qualitative changes in the phase portrait. The derived solutions are depicted via contour plots, along with two-dimensional (2D) and three-dimensional (3D) representations, utilizing Mathematica for computational validation and graphical illustration. This study is motivated by the growing role of fractional calculus in modeling nonlinear wave phenomena where memory and hereditary effects cannot be captured by classical integer-order approaches. The time-fractional Biswas–Arshed (BA) equation is investigated to obtain diverse soliton solutions using the Extended Simplest Equation Method (ESEM) under the β-derivative and M-truncated derivative operators. Beyond solution construction, a nonlinear second-order equation is reformulated as a planar dynamical system to analyze its bifurcation and stability properties. This dual approach highlights how parameter variations affect equilibrium structures and soliton behaviors, offering both theoretical insights and potential applications in physics and engineering.

Keywords: extended simplest equation method (ESEM); bifurication analysis; exact solutions; solitons; time-fractional Biswas–Arshed (BA) model; β and M-truncated fractional derivatives

MSC: 35C07; 35C07; 83C15

check for updates

Academic Editor: Fengping Yao

Received: 3 September 2025
Revised: 22 September 2025
Accepted: 23 September 2025
Published: 1 October 2025

Citation: Zafar, A.; Razzaq, W.; Nazir, A.; Alomair, M.A.; Al Naim, A.S.; Alomair, A. Bifurcation Analysis and Solitons Dynamics of the Fractional Biswas–Arshed Equation via Analytical Method. *Mathematics* **2025**, *13*, 3147. https://doi.org/10.3390/math13193147

Copyright: © 2025 by the authors. Licensee MDPI, Basel, Switzerland. This article is an open access article distributed under the terms and conditions of the Creative Commons Attribution (CC BY) license (https://creativecommons.org/licenses/by/4.0/).

1. Introduction

Fractional calculus has fascinated many specialists due to its implications in uncovering deeper aspects of present reality. Although fractional derivatives were introduced nearly three centuries ago, they were not entirely a new concept [1]. Recent research on nonlinear fractional partial differential equations (NLFPDEs) has risen significantly, highlighting their diverse applications across various domains, including engineering, medical fields, controlled thermonuclear fusion, plasma physics, stochastic dynamical processes, acoustics, diffusive transport, chemical physics, solid state physics, electric networks, astrophysics, electromagnetic theory, fluid mechanics, geochemistry, fractional dynamics, manipulation theory, chemical kinematics, system identification, biogenetics, optical fibers, and many others [2–5]. The above-mentioned topics are closely related to engineering concepts such as response, diffusion, convection, and dispersion, and NLFPDEs can be applied to accurately solve them. Fractional calculus is the principal technique for differentiating and integrating averages of any order, enabling the construction and understanding of various physical features associated with continuous transitions from stationary to oscillatory phenomena. Due to the prevalence of fractional nonlinear differential equations (FNLDEs) throughout several engineering and scientific fields, numerous researchers focus their efforts on deriving exact or approximate solutions to these dynamic FNLDEs. Ahmed et al. [6] derive a rational solution, singular-periodic wave, periodic wave solution, dark, and collective dark–bright solutions of space-time NLFE for communication lines via the improved generalized Riccati equation technique.The single-wave solutions of the generalized Rosenau–Korteweg-de Vries (RKDv) regularized long-wave model were examined by Avazzadeh et al. [7]. Asjad et al. [8] examined nonlinear differential time-fractional equation to derive solutions like trigonometric functions, exponential functions, rational functions, and hyperbolic functions utilizing the EDA approach. Zaman et al. [9] investigated nonlinear fractional Allen Cahn (AC) and space-time Phi-4 equations via $(\frac{G'}{G})$-expansion technique to obtain periodic soliton, singular kink, dynamical compaction, and single soliton-type solutions. Sadiya et al. [10] derived single solitons, kink type, bell shape, double solitons and multiple solitons types results by applying tanh-function technique to the Klein–Gordon and nonlinear time-fractional Sine-Gordon (SG) model. To analyze coupled approximate-long-water wave and space-time nonlinear fractional coupled systems, Zaman et al. [11] implemented the tanh-function method. To derive soliton solutions, such as bell-shape and kink-type solutions, use the Whitham–Broer–Kaup equation. Arefin et al. [12] utilized the Riemann–Liouville fractional derivative along with the two-variable $(\frac{G'}{G}, \frac{1}{G})$-expansion technique to obtain exact solutions for the space-time NLF (2 + 1)-dimensional diffusive long-wave equation and the approximated long water-wave equation. During the application of the fractional differential sub-equation technique. RASHED et al. [13] examined the space-time NLF differential modified Benjamin Bona-Mahony model. Furthermore, two-variable $(\frac{G'}{G}, \frac{1}{G})$-expansion technique [14,15], Sine–Gordon expansion method [16], $(\frac{G'}{G^2})$-expansion technique [17], modified extended tanh function approach [18], sine cosine and sinh cosh method [19], a novel modified extended direct algebraic method [20], extended generalized Riccati equation mapping method [21], Paul–Painlevé method [22], Laplace Pade–Caputo-fractional differential transform technique [23], generalized Kudryashov technique [24], explicit finite-difference technique [25], the Yang decomposition technique and homotopy perturbation technique [26], optimized decomposition technique [27], Chelyshkov wavelets method [28], differential inequality technique and integral transformation method [29], hybrid local fractional approach [30], natural decomposition technique [31], Mohand variational iteration transform technique and novel approximate analytical technique [32], iterative method [33], fractional new

analytic technique [34], F-expansion approach [35], Elzaki transform technique [36], Adomia -decomposition and Jafari transform technique [37], Laplace residual power series approach [38], Bernstein spectral approach [39] are adopted by different researchers to solve NFFDEs. Here, our concern is to solve the Biswas arshed (BA) equation. Biswas and Arshed [40] introduced an innovative concept aimed at reducing issues by attaining an optimal equilibrium between dispersion and nonlinearity to preserve solitons in metamaterials, crystal fibers, optical fibers, and photonic crystal fibers, possibly leading to reduced group velocity dispersion and an absence of nonlinearity. In this instance, they recovered the combo, bright, and singular solitons to demonstrate that solitons still exist for BA equation. Many researchers have recently provided an explanation of the BA equation. Alhojilan et al. [41] find stochastic bright solutions, stochastic dark solutions, stochastic singular solutions, stochastic rational solution, stochastic singular-bright solutions, stochastic periodic solutions, and stochastic bright-dark solutions by investigating the Biswas–Arshed equation via modified extended mapping technique. Cinar et al. [42] used an extended sine cosine approach and extended sinh-cosh approach and obtain singular solitons solutions, dark solitons solutions, and singular-periodic soliton solutions from Biswas Arshed equation. Zhao Li et al. [43] obtain optical and traveling wave solitons solutions by investigating the BA equation including beta-derivative via Li's three-step technique. Ghazala et al. [44] formed trigonometric function solutions, rational function solutions and hyperbolic function solutions by investigating BA model through the improved auxiliary equation method. Akbulut and Rayhanul [45] applied improved extended auxiliary equation and improved F-expansion technique to BA equation, including the β-derivative to gain rational function solutions, trigonometric function solutions, and hyperbolic function solutions. Sachin and Monika [46] investigated BA equation via a generalized exponential-rational function method and kudryashov's technique to extract solitons solutions.

The governing model has the following form:

$$ij_t + a_1 j_{xx} + a_2 j_{xt} + i(b_1 j_{xxx} + b_2 j_{xxt}) = i[\delta(|j|^2 j)_x + \mu(|j|^2)_x j + \lambda |j|^2 j_x], \tag{1}$$

where $j(x,t)$ rely on x and t characterizes soliton profile, x represents the distance and t represents the time variables. a_1 represents the group velocity dispersion (GVD), while a_2, b_1 are the spatio-temporal dispersion coefficient and b_2 for the third-order dispersion coefficient. The nonlinearity is defined by the third component in the equation on the right-hand side, where δ denotes the influence of self-steepening, while λ and μ indicate the nonlinear dispersion effect. Another powerful technique has been offered by Kudryashov in his research [47,48], the simplest equation technique is the name given to this methodology. Recently, Bilige et al. [49,50] modified this technique which is named the modified simplest equation technique. Subsequently, numerous researchers [51,52] applied this technique to gain novel exact solitons solutions for NLPDEs. This study uses extended-simplest equation technique to find new trigonometric, hyperbolic, and rational solutions for the BA equation and explains the resulting solutions, which include the β-derivative and M-truncated by their graphical representations. In this paper, We conduct a comprehensive comparison of the β and M-truncated fractional derivatives applied to the Biswas–Arshed equation utilizing the Extended Simplest Equation technique. Unlike earlier research, which focused primarily on individual fractional derivatives or conventional analytical approaches, ours uniquely mixes beta and M-truncated derivatives within the same framework. This makes a direct comparative study, which the literature has not yet extensively investigated, feasible. Furthermore, we derive a more general and effective solution method, thereby generating a class of soliton solutions. This study offers innovative analytical perspectives that surpass prior research and elucidates the progression of fractional derivatives in nonlinear equa-

tions. This facilitates future progress in fractional calculus and its applications in complex physical systems.

This paper is organized as follows: Preliminaries are outlined in Section 2. The proposed approaches are summarized in Section 3. The governing models are outlined in Section 4. Section 5 discusses the application of the proposed methodologies to the governing system for extracting precise solutions. Section 6 presents graphical representations of several findings. Bifurcation analysis are described in Section 7. Section 8 contains the presentation of the conclusion and future work.

2. Preliminaries

2.1. β-Derivative

Definition 1 (Atangana et al. [53]). *Let $u(z)$ be a function that is defined for any non-negative z. Therefore, the β-derivative of $u(z)$ is as follows:*

$$T^{\beta}(u(z)) = \frac{d^{\beta}u(z)}{dz^{\beta}} = \lim_{\xi \to 0} \frac{u\left(z + \xi\left(z + \frac{1}{\Gamma(\beta)}\right)^{1-\beta}\right) - u(z)}{\xi}, \ 1 < \beta \leq 1. \tag{2}$$

Theorem 1. *Let $u(z)$ and $v(z)$ be β-differentiable functions for all $z > 0$ and $\beta \in (0, 1]$ (Martínez et al. [54]). Then,*

$$T^{\beta}(ru(z) + sv(z)) = rT^{\beta}(u(z)) + sT^{\beta}(v(z)), \forall r, s \in \mathbb{R}.$$

$$T^{\beta}(u(z)v(z)) = v(z)T^{\beta}(u(z)) + u(z)T^{\beta}(v(z)).$$

$$T^{\beta}\left(\frac{u(z)}{v(z)}\right) = \frac{v(z)T^{\beta}(u(z)) - u(z)T^{\beta}(v(z))}{v^2(z)}.$$

$$T^{\beta}(u(z)) = \left(z + \frac{1}{\Gamma(\beta)}\right)^{1-\beta} \frac{du(z)}{dz}.$$

2.2. M-Truncated Derivative

Definition 2. *The Truncated-Mittag–Leffler function [55] is defined as follows:*

$${}_i\mathbb{E}_{\beta}(g(z)) = \sum_{m=0}^{i} \frac{g(z)^m}{\Gamma(\beta m + 1)}, \tag{3}$$

where $g \in \mathbb{C}$ and $\beta > 0$

Definition 3. *Let v: $[0, \infty) \to R$ be a function. The M-truncated derivative of v of order γ, where $\gamma \in (0, 1)$ with respect to z, is defined as*

$$\mathbb{D}_{(M,z)}^{(\gamma,\beta)} v(z) = \lim_{h \to 0} \frac{v(z + {}_i\mathbb{E}_{\beta}(hz^{-\beta})) - v(z)}{h}, \beta, z > 0, \tag{4}$$

where ${}_i\mathbb{E}_{\beta}(.)$ is the truncated Mittag–Leffler function.

Theorem 2. *Let us assume that $0 < \gamma \leq 1, p, q \in \mathbb{R}$, $\beta > 0$, ψ and φ be a γ-diferentiable at any $z > 0$. Then,*

$$\mathbb{D}_{(M,z)}^{(\gamma,\beta)}(p\psi + q\varphi)(z) = p\mathbb{D}_{(M,z)}^{(\gamma,\beta)}\psi(z) + q\mathbb{D}_{(M,z)}^{(\gamma,\beta)}\varphi(z), \ p, q \in \mathbb{R}.$$

$$\mathbb{D}_{(M,z)}^{(\gamma,\beta)}(\psi\varphi)(z) = \psi(z)\mathbb{D}_{(M,z)}^{(\gamma,\beta)}\varphi(z) + \varphi(z)\mathbb{D}_{(M,z)}^{(\gamma,\beta)}\psi(z).$$

$$\mathbb{D}^{(\gamma,\beta)}_{(M,z)}\left(\frac{\psi}{\varphi}\right)(z) = \frac{\psi(z)\mathbb{D}^{(\gamma,\beta)}_{(M,z)}\varphi(z) - \varphi(z)\mathbb{D}^{(\gamma,\beta)}_{(M,z)}\psi(z)}{\varphi(z)^2}.$$

If ψ is diferentiable, then

$$\mathbb{D}^{(\gamma,\beta)}_{(M,z)}(\psi)(z) = \frac{z^{1-\gamma}}{\Gamma(\beta+1)}\frac{d\psi(z)}{dz}.$$

3. Description of the Method

To explain this method, initially consider the following projective Riccati equation:

$$f'(\chi) = -f(\chi)g(\chi),\ \ g'(\chi) = -g^2(\chi) + \sigma f(\chi) - \rho,\ \ \rho \neq 0 \tag{5}$$

where ρ and σ are constants. Consider

$$f(\chi) = \frac{1}{\phi(\chi)},\ \ g(\chi) = \frac{\phi'(\chi)}{\phi(\chi)},\ \ \phi(\chi) \neq 0 \tag{6}$$

$\phi(\chi)$ is the result of the following ODE of order two.

$$\sigma = \phi''(\chi) + \rho\phi(\chi). \tag{7}$$

For this ODE, there are three different kinds of solutions.

(1) **For $\rho < 0$,** hyperbolic function solution exist:

$$\phi(\chi) = B_1 cosh\left(\chi\sqrt{-\rho}\right) + B_2 sinh\left(\chi\sqrt{-\rho}\right) + \frac{\sigma}{\rho}. \tag{8}$$

Due to this,

$$\left(\frac{\phi'(\chi)}{\phi(\chi)}\right)^2 - \Delta_1\left(\frac{1}{\phi(\chi)}\right) - \frac{2\sigma}{\phi(\chi)} + \rho = 0, \tag{9}$$

where, $\Delta_1 = \rho B_1^2 - \rho B_2^2 - \frac{\sigma^2}{\rho}$

(2) **For $\rho > 0$,** trigonometric function solution exist:

$$\phi(\chi) = B_1 cos(\chi\sqrt{\rho}) + B_2 sin(\chi\sqrt{\rho}) + \frac{\sigma}{\rho}. \tag{10}$$

Due to this,

$$\left(\frac{\phi'(\chi)}{\phi(\chi)}\right)^2 - \Delta_2\left(\frac{1}{\phi(\chi)}\right) - \frac{2\sigma}{\phi(\chi)} + \rho = 0, \tag{11}$$

where, $\Delta_2 = \rho B_1^2 - \rho B_2^2 - \frac{\sigma^2}{\rho}$

(3) **For $\rho = 0$,** the solution is as follows:

$$\phi(\chi) = \frac{\sigma\chi^2}{2} + B_1\chi + B_2. \tag{12}$$

Due to this,

$$\left(\frac{\phi'(\chi)}{\phi(\chi)}\right)^2 - \Delta_3\left(\frac{1}{\phi(\chi)}\right) - \frac{2\sigma}{\phi(\chi)} = 0, \tag{13}$$

where, $\Delta_3 = B_1^2 - 2\sigma B_2$.

Here, B_1 and B_2 are arbitrary constants.

Examine the nonlinear $(n+1)$-dimensional partial differential equation (PDE)

$$H(j, j_x, j_t, j_{xx}, j_{xt}, j_{tt}, \ldots) = 0, \tag{14}$$

where F is a polynomial in $j(x,t)$ and its partial derivatives, containing the highest order derivatives and the nonlinear terms.

The key components of this methodology are outlined as follows:
Stage (1): With the aid of a traveling wave theory.

$$j(x,t) = J(\chi)e^{i\chi}, \chi = x - \frac{\tau}{\beta}\left(\frac{1}{\Gamma(\beta)} + t\right)^{\beta}, \eta = -dx + \frac{v}{\beta}\left(\frac{1}{\Gamma(\beta)} + t\right)^{\beta} + \epsilon.$$

$$j(x,t) = J(\chi)e^{i\eta}, \chi = x - \frac{\tau\Gamma(\beta+1)t^{\gamma}}{\gamma}, \eta = -dx + \frac{v\Gamma(\beta+1)t^{\gamma}}{\gamma} + \epsilon. \tag{15}$$

The traveling wave theory transforms (15) the nonlinear PDE (14) into the nonlinear ODE as follows

$$\mathbb{G}(j, j', j'', \ldots) = 0, \tag{16}$$

where $\mathbb{G}$ is a polynomial in $j(\chi)$ and its total derivative with respect to χ.
Stage (2): Assume the following solution to Equation (16).

$$j(\chi) = \sum_{i=0}^{M} \alpha_i \left[\frac{\phi'(\chi)}{\phi(\chi)}\right]^i + \sum_{j=0}^{M-1} \beta_j \left[\frac{\phi'(\chi)}{\phi(\chi)}\right]^i \frac{1}{\phi(\chi)}, \tag{17}$$

where $\phi(\chi)$ is the solution of second order ODE (7) and α_i and β_j are arbitrary constants.
Stage (3): By substitution (7), (9), (11), (13), and (17) to Equation (16), collect all terms with the same order of $\left(\frac{1}{\phi^i(\chi)}\right)$ and $\left(\frac{1}{\phi^j(\chi)}\right)\left(\frac{\phi'(\chi)}{\phi(\chi)}\right)$ together and a set of algebraic equations results from setting them to zero. Find ρ, σ, α_i, β_i a_1, a_2, b_1, b_2 by solving this system with the aid of Mathematica.

4. Governing Models

In this part, define the governing model equations including both β derivatives and M-truncated derivatives.

4.1. Biswas Arshed Equation Including β-Derivative

Han T. et al. [56] defined BA equation including β-derivative as

$$i\frac{\partial^{\beta} j}{\partial t^{\beta}} + a_1\frac{\partial^2 j}{\partial x^2} + a_2\frac{\partial^{\beta}}{\partial t^{\beta}}\left(\frac{\partial j}{\partial x}\right) - i\left(\delta\frac{\partial |j|^2 j}{\partial x} + \mu j\frac{\partial |j|^2}{\partial x} + \lambda |j|^2\frac{\partial j}{\partial x}\right)$$

$$+i\left(b_1\frac{\partial^3 j}{\partial x^3} + b_2\frac{\partial^{\beta}}{\partial t^{\beta}}\left(\frac{\partial^2 j}{\partial x^2}\right)\right) = 0,\ 0 < \beta \leq 1, \tag{18}$$

where i represent the imaginary part, j is the function of x and t, $\frac{\partial^{\beta}}{\partial t^{\beta}}$ is the operator for β-derivative, β represents fractional order, a_1, a_2, b_1, and b_2 are arbitrary constants, δ, μ, and λ are nonzero parameters, the wave transformations listed below will be used:

$$j(x,t) = J(\chi)e^{i\eta},\ \chi = x - \frac{\tau}{\beta}\left(\frac{1}{\Gamma(\beta)} + t\right)^{\beta},\ \eta = -dx + \frac{v}{\beta}\left(\frac{1}{\Gamma(\beta)} + t\right)^{\beta} + \epsilon, \tag{19}$$

where η , v, τ, and ϵ are non-zero parameters.

4.2. Biswas Arshed Equation Including M-Truncated Derivative

$$i\mathbb{D}_{(M,z)}^{(\gamma,\beta)}(j)+a_1\frac{\partial^2 j}{\partial x^2}+a_2\mathbb{D}_{(M,z)}^{(\gamma,\beta)}\left(\frac{\partial j}{\partial x}\right)-i\left(\delta\frac{\partial|j|^2 j}{\partial x}+\mu j\frac{\partial|j|^2}{\partial x}+\lambda|j|^2\frac{\partial j}{\partial x}\right)$$
$$+i\left(b_1\frac{\partial^3 j}{\partial x^3}+b_2\mathbb{D}_{(M,z)}^{(\gamma,\beta)}\left(\frac{\partial^2 j}{\partial x^2}\right)\right)=0,\ 0<\gamma\leq 1,\ \beta>0, \tag{20}$$

where i represent the imaginary part, J is the function of x and t, $\mathbb{D}_{(M,z)}^{(\gamma,\beta)}$ is operator for the γ-derivative, γ represents fractional order, a_1, a_2, b_1, and b_2 are arbitrary constants, δ, μ, and λ are nonzero parameters, the wave transformations listed below will be used:

$$j(x,t)=J(\chi)e^{i\eta}, \chi=x-\frac{\tau\Gamma(\beta+1)t^\gamma}{\gamma}, \eta=-dx+\frac{\upsilon\Gamma(\beta+1)t^\gamma}{\gamma}+\epsilon, \tag{21}$$

where η, υ, τ, and ϵ are non-zero parameters. In this study, we considered fractional operators defined on the whole memory interval [0, T]. However, in many real-world systems, distant past effects gradually diminish, and it is more realistic to restrict the fractional operator to a finite memory horizon, often referred to as the "short-memory principle." In such cases, the fractional kernel is truncated so that only the most recent history contributes to the system's dynamics. This concept has been shown to provide accurate models for viscoelastic and structural materials with fading memory effects [57,58]. Extending the Biswas–Arshed model to incorporate short-memory operators would therefore be an interesting future direction, offering a balance between computational efficiency and physical realism. The parameters β and γ represent the fractional orders in the β-derivative and the M-truncated derivative, respectively. Physically, these parameters quantify the extent of memory and hereditary effects in the system. When $\beta = 1$ (or $\gamma = 1$), the model reduces to the classical integer-order form without memory. For $0 < \beta, \gamma < 1$, the model incorporates anomalous diffusion and long-range temporal correlations. Smaller values correspond to stronger memory effects, where past states significantly influence present dynamics, while larger values closer to unity indicate weaker memory and near-classical behavior. In the case of the M-truncated operator, γ also introduces a tempered Mittag–Leffler kernel that effectively restricts the memory influence, making it particularly suitable for systems with fading memory such as viscoelastic materials oranomalous transport with cutoff effects.

5. Applications

This section employs the extended simplest equation method to resolve the Biswas–Arshed equation, including both β and M-truncated derivatives. By substituting the wave transformations specified in (19) and (21) into (18) and (20), the resulting nonlinear ordinary differential equations are derived by separating the imaginary and real components, respectively.

$$(b_1-b_2\tau)J^{(3)}(\chi)+J'(\chi)(d(a_2\tau-2a_1+2b_2\upsilon)+a_2\upsilon+d^2(b_2\tau-3b_1)-\tau)$$
$$-(J(\chi))^2(\eta+3\delta+2\mu)J'(\chi)=0. \tag{22}$$
$$J''(\chi)(a_1-a_2\tau-2b_2d\tau+3b_1d-b_2\upsilon)-(J(\chi))^3d(\eta+\delta)$$
$$+J(\chi)(\upsilon(a_2d+b_2d^2-1)-a_1d^2-b_1d^3)=0. \tag{23}$$

The following are the constraint conditions that can be found from Equation (22)

$$\tau=\frac{b_1}{b_2}, \delta=-\frac{1}{3}(\eta+2\mu), \upsilon=-\frac{a_2b_1d-2a_1b_2d-2b_1b_2d^2-b_1}{b_2(a_2+2b_2d)}. \tag{24}$$

Inserting Equation (24) into Equation (23)

$$d_1 J''(\chi) + d_2 J(\chi) + d_3 (J(\chi))^3 = 0, \tag{25}$$

where

$$\begin{aligned} d_1 &= -\frac{a_2 b_1}{b_2} + a_1 + b_1 d + d_4, \\ d_2 &= -\frac{a_2 d_4 d}{b_2} - a_1 d^2 + \frac{d_4}{b^2} - b_1 d^3 - d_4 d^2, \\ d_3 &= -\lambda d + \frac{1}{3} d(\lambda + 2\mu), \\ d_4 &= \frac{a_2 b_1 d - 2a_1 b_2 d - 2b_1 b_2 d^2 - b_1}{a_2 + 2b_2 d}. \end{aligned}$$

Equation (25) is used to determine the homogeneous balance number through the terms $J''(\chi)$ and $(J(\chi))^3$, we got M = 1 and the following formal solution from Equation (25).

$$J(\chi) = \frac{\alpha_1 \phi'(\chi)}{\phi(\chi)} + \alpha_0 + \frac{\beta_0}{\phi(\chi)}. \tag{26}$$

Type 1. **For** $\rho < 0$**.**

Substitute Equation (26) with the linear OD Equation (7) and relation (9) into Equation (25), accumulate all the expression with the identical power of $\left(\frac{1}{\phi^i(\chi)}\right)$ and $\left(\frac{1}{\phi^j(\chi)}\right)\left(\frac{\phi'(\chi)}{\phi(\chi)}\right)$ and put them equal to zero, the system of algebraic equations below is obtained.

Utilizing MATHEMATICA to resolve these nonlinear algebraic equations obtains the results given below:

Result:

$$\left\{ \begin{aligned} \alpha_0 = 0, \alpha_1 = \pm \frac{\sqrt{\frac{3}{2}}\sqrt{b_1}}{\sqrt{2a_2 b_2 \lambda d^3 - 2a_2 b_2 d^3 \mu + a_2 b_2 \rho \lambda d - a_2 b_2 \rho d \mu - 4b_2 \lambda d^2 + 4b_2 d^2 \mu}}, \\ \beta_0 = \pm \frac{\sqrt{\frac{3}{2}}\sqrt{b_1}\sqrt{\Delta_1}}{\sqrt{2a_2 b_2 \lambda d^3 - 2a_2 b_2 d^3 \mu + a_2 b_2 \rho \lambda d - a_2 b_2 \rho d \mu - 4b_2 \lambda d^2 + 4b_2 d^2 \mu}}, \\ a_1 = \frac{b_1 (a_2^2 \rho + 2a_2^2 d^2 - 4a_2 d + b_2 \rho + 2b_2 d^2 + 2)}{b_2 (a_2 \rho + 2a_2 d^2 - 4d)} \end{aligned} \right\} \tag{27}$$

From Equations (8), (15), (26) and (27), obtain the hyperbolic solution of Equation (1) as follows:

For β-derivative:

$$J(x,t) = \left(\frac{\pm\sqrt{b_1}\sqrt{\frac{3}{2}}}{\sqrt{2a_2 b_2 \lambda d^3 - 2a_2 b_2 d^3 \mu + a_2 b_2 \rho \lambda d - a_2 b_2 \rho d \mu - 4b_2 \lambda d^2 + 4b_2 d^2 \mu}} \right) \left(\sqrt{-\rho}\vartheta_1(\chi) + \sqrt{\Delta_1}\vartheta_1(\chi) \right) e^{-dx + \frac{v}{\beta}\left(\frac{1}{\Gamma(\beta)} + t\right)^{\beta} + \epsilon}, \tag{28}$$

where

$$\vartheta_1(\chi) = \frac{B_1 \sinh(\chi\sqrt{-\rho}) + B_2 \cosh(\chi\sqrt{-\rho})}{B_1 \cosh(\chi\sqrt{-\rho}) + B_2 \sinh(\chi\sqrt{-\rho}) + \frac{\sigma}{\rho}},$$

$$\vartheta_2(\chi) = \frac{1}{B_1 \cosh(\chi\sqrt{-\rho}) + B_2 \sinh(\chi\sqrt{-\rho}) + \frac{\sigma}{\rho}}.$$

In particular, if set $B_1 = 0, B_2 \neq 0, \sigma = 0$ in Equation (28), obtain singular wave solution

$$J(x,t) = \left(\frac{\pm\sqrt{b_1}\sqrt{\frac{3}{2}}}{\sqrt{2a_2b_2\lambda d^3 - 2a_2b_2d^3\mu + a_2b_2\rho\lambda d - a_2b_2\rho d\mu - 4b_2\lambda d^2 + 4b_2d^2\mu}} \right)$$

$$\left(\coth\left(\sqrt{-\rho}\chi\right) + \operatorname{csch}\left(\sqrt{-\rho}\chi\right)\right) e^{-dx + \frac{v}{\beta}\left(\frac{1}{\Gamma(\beta)} + t\right)^{\beta} + \epsilon}, \tag{29}$$

For M-truncated derivative:

$$J(x,t) = \left(\frac{\pm\sqrt{b_1}\sqrt{\frac{3}{2}}}{\sqrt{2a_2b_2\lambda d^3 - 2a_2b_2d^3\mu + a_2b_2\rho\lambda d - a_2b_2\rho d\mu - 4b_2\lambda d^2 + 4b_2d^2\mu}} \right)$$

$$\left(\sqrt{-\rho}\vartheta_1(\chi) + \sqrt{\Delta_1}\vartheta_2(\chi)\right) e^{-dx + \frac{v\Gamma(\beta+1)t^{\gamma}}{\gamma} + \epsilon}, \tag{30}$$

where

$$\vartheta_1(\chi) = \frac{B_1\sinh(\chi\sqrt{-\rho}) + B_2\cosh(\chi\sqrt{-\rho})}{B_1\cosh(\chi\sqrt{-\rho}) + B_2\sinh(\chi\sqrt{-\rho}) + \frac{\sigma}{\rho}},$$

$$\vartheta_2(\chi) = \frac{1}{B_1\cosh(\chi\sqrt{-\rho}) + B_2\sinh(\chi\sqrt{-\rho}) + \frac{\sigma}{\rho}}.$$

In particular, if set $B_1 = 0, B_2 \neq 0, \sigma = 0$ in Equation (30), obtain singular wave solution

$$J(x,t) = \left(\frac{\pm\sqrt{\frac{3}{2}}\left(\sqrt{b_1}\sqrt{-\rho}\right)}{\sqrt{2a_2b_2\lambda d^3 - 2a_2b_2d^3\mu + a_2b_2\rho\lambda d - a_2b_2\rho d\mu - 4b_2\lambda d^2 + 4b_2d^2\mu}} \right)$$

$$\left(\coth\left(\sqrt{-\rho}\chi\right) + \operatorname{csch}\left(\sqrt{-\rho}\chi\right)\right) e^{-dx + \frac{v\Gamma(\beta+1)t^{\gamma}}{\gamma} + \epsilon}. \tag{31}$$

Type 2. **For** $\rho > 0$**.**

Substitute Equation (26) with the linear OD Equation (7), and relation (11) into Equation (25), accumulate all the expression with the identical power of $\left(\frac{1}{\phi^i(\chi)}\right)$ and $\left(\frac{1}{\phi^j(\chi)}\right)\left(\frac{\phi'(\chi)}{\phi(\chi)}\right)$ and put them equal to zero, the system of algebraic equations below is obtained.

By using Mathematica to solve these nonlinear algebraic equations and obtain results are shown below.

Result:

$$\left\{ \begin{array}{c} \alpha_0 = 0, \alpha_1 = \pm\dfrac{\sqrt{\frac{3}{2}}\sqrt{b_1}}{\sqrt{2a_2b_2\lambda d^3 - 2a_2b_2d^3\mu + a_2b_2\rho\lambda d - a_2b_2\rho d\mu - 4b_2\lambda d^2 + 4b_2d^2\mu}}, \\ \beta_0 = \pm\dfrac{\sqrt{\frac{3}{2}}\sqrt{b_1}\sqrt{\Delta_2}}{\sqrt{2a_2b_2\lambda d^3 - 2a_2b_2d^3\mu + a_2b_2\rho\lambda d - a_2b_2\rho d\mu - 4b_2\lambda d^2 + 4b_2d^2\mu}}, \\ a_1 = \dfrac{b_1\left(a_2^2\rho + 2a_2^2d^2 - 4a_2d + b_2\rho + 2b_2d^2 + 2\right)}{b_2(a_2\rho + 2a_2d^2 - 4d)} \end{array} \right\} \tag{32}$$

From Equations (10), (15), (26) and (32), obtain the trigonometric solution of Equation (1) as follows:

For β-derivative:

$$J(x,t) = \left(\frac{\pm\sqrt{b_1}\sqrt{\frac{3}{2}}}{\sqrt{2a_2b_2\lambda d^3 - 2a_2b_2d^3\mu + a_2b_2\rho\lambda d - a_2b_2\rho d\mu - 4b_2\lambda d^2 + 4b_2d^2\mu}} \right)$$

$$\left(\sqrt{\rho}\vartheta_1(\chi)+\sqrt{\Delta_2}\vartheta_2(\chi)\right)e^{-dx+\frac{v}{\beta}\left(\frac{1}{\Gamma(\beta)}+t\right)^{\beta}+\epsilon}, \tag{33}$$

where

$$\vartheta_1(\chi)=\frac{-B_1\sin(\chi\sqrt{\rho})+B_2\cos(\chi\sqrt{\rho})}{B_1\cos(\chi\sqrt{\rho})+B_2\sin(\chi\sqrt{\rho})+\frac{\sigma}{\rho}},$$

$$\vartheta_2(\chi)=\frac{1}{B_1\cos(\chi\sqrt{\rho})+B_2\sin(\chi\sqrt{\rho})+\frac{\sigma}{\rho}}.$$

In particular, if set $B_1=0, B_2\neq 0, \sigma=0$, Equation (33) and obtain periodic wave solution

$$J(x,t)=\left(\frac{\pm\sqrt{b_1}\sqrt{\frac{3}{2}}}{\sqrt{2a_2b_2\lambda d^3-2a_2b_2d^3\mu+a_2b_2\rho\lambda d-a_2b_2\rho d\mu-4b_2\lambda d^2+4b_2d^2\mu}}\right)$$

$$(\cot(\sqrt{\rho}\chi)+\csc(\sqrt{\rho}\chi))e^{-dx+\frac{v}{\beta}\left(\frac{1}{\Gamma(\beta)}+t\right)^{\beta}+\epsilon}. \tag{34}$$

In particular, if set $B_1\neq 0, B_2=0, \sigma=0$, Equation (33) and obtain periodic wave solution

$$J(x,t)=\left(\frac{\pm\sqrt{b_1}\sqrt{\frac{3}{2}}}{\sqrt{2a_2b_2\lambda d^3-2a_2b_2d^3\mu+a_2b_2\rho\lambda d-a_2b_2\rho d\mu-4b_2\lambda d^2+4b_2d^2\mu}}\right)$$

$$(\tan(\sqrt{\rho}\chi)-\sec(\sqrt{\rho}\chi))e^{-dx+\frac{v}{\beta}\left(\frac{1}{\Gamma(\beta)}+t\right)^{\beta}+\epsilon}, \tag{35}$$

For M-truncated derivative:

$$J(x,t)=\left(\frac{\pm\sqrt{b_1}\sqrt{\frac{3}{2}}}{\sqrt{2a_2b_2\lambda d^3-2a_2b_2d^3\mu+a_2b_2\rho\lambda d-a_2b_2\rho d\mu-4b_2\lambda d^2+4b_2d^2\mu}}\right)$$

$$\left(\sqrt{\rho}\vartheta_1(\chi)+\sqrt{\Delta_2}\vartheta_2(\chi)\right)e^{-dx+\frac{v\Gamma(\beta+1)t^{\gamma}}{\gamma}+\epsilon}, \tag{36}$$

where

$$\vartheta_1(\chi)=\frac{-B_1\sin(\chi\sqrt{\rho})+B_2\cos(\chi\sqrt{\rho})}{B_1\cosh(\chi\sqrt{\rho})+B_2\sinh(\chi\sqrt{-\rho})+\frac{\sigma}{\rho}},$$

$$\vartheta_2(\chi)=\frac{1}{B_1\cos(\chi\sqrt{\rho})+B_2\sin(\chi\sqrt{\rho})+\frac{\sigma}{\rho}}.$$

In particular, if set $B_1=0, B_2\neq 0, \sigma=0$, Equation (36), obtain periodic wave solution

$$J(x,t)=\left(\frac{\pm\sqrt{\frac{3}{2}}(\sqrt{b_1}\sqrt{\rho})}{\sqrt{2a_2b_2\lambda d^3-2a_2b_2d^3\mu+a_2b_2\rho\lambda d-a_2b_2\rho d\mu-4b_2\lambda d^2+4b_2d^2\mu}}\right)$$

$$(\cot(\sqrt{\rho}\chi)+\csc(\sqrt{\rho}\chi))e^{-dx+\frac{v\Gamma(\beta+1)t^{\gamma}}{\gamma}+\epsilon}. \tag{37}$$

In particular, if set $B_1\neq 0, B_2=0, \sigma=0$, Equation (36) and obtain periodic wave solution

$$J(x,t)=\left(\frac{\pm\sqrt{\frac{3}{2}}(\sqrt{b_1}\sqrt{\rho})}{\sqrt{2a_2b_2\lambda d^3-2a_2b_2d^3\mu+a_2b_2\rho\lambda d-a_2b_2\rho d\mu-4b_2\lambda d^2+4b_2d^2\mu}}\right)$$

$$(\tan(\sqrt{\rho}\chi)-\sec(\sqrt{\rho}\chi))e^{-dx+\frac{v\Gamma(\beta+1)t^{\gamma}}{\gamma}+\epsilon}. \tag{38}$$

Type 3. **For** $\rho = 0$**.**

Substitute Equation (26) with the linear OD Equation (7), and relation (13) into Equation (25), accumulate all the expression with the identical power of $\left(\frac{1}{\phi^i(\chi)}\right)$ and $\left(\frac{1}{\phi^j(\chi)}\right)\left(\frac{\phi'(\chi)}{\phi(\chi)}\right)$ and put them equal to zero, the system of algebraic equations below is obtained.

$$\begin{aligned}
\left(\frac{1}{\phi(\chi)}\right)^0 &: -\frac{1}{3}\alpha_0 d\left(2\alpha_0^2(\lambda-\mu)+3a_1 d+3b_1 d^2\right)\\
&\quad +\frac{\alpha_0\left(a_2 d+b_2 d^2-1\right)\left(b_1\left(-a_2 d+2b_2 d^2+1\right)+2a_1 b_2 d\right)}{b_2(a_2+2b_2 d)}=0,\\
\left(\frac{1}{\phi(\chi)}\right) &: -d\left(\beta_0 d(a_1+b_1 d)+2\alpha_0^2\beta_0(\lambda-\mu)+4\alpha_1^2\alpha_0\sigma(\lambda-\mu)\right)\\
&\quad +\frac{\beta_0\left(a_2 d+b_2 d^2-1\right)\left(b_1\left(-a_2 d+2b_2 d^2+1\right)+2a_1 b_2 d\right)}{b_2(a_2+2b_2 d)}=0,\\
\left(\frac{1}{\phi(\chi)}\right)^2 &: 3a_1\beta_0\sigma+d\left(3b_1\beta_0\sigma-2(\lambda-\mu)\left(\alpha_1^2(\alpha_0\Delta_3+2\beta_0\sigma)+\alpha_0\beta_0^2\right)\right)\\
&\quad -\frac{3\beta_0\sigma\left(b_2\left(2a_1 b_2 d+b_1\left(2b_2 d^2+1\right)\right)+a_2 b_1 b_2 d+a_2^2 b_1\right)}{b_2(a_2+2b_2 d)}=0,\\
\left(\frac{1}{\phi(\chi)}\right)^3 &: \frac{1}{3}(-2)\beta_0\left(\beta_0^2 d(\lambda-\mu)-3\Delta_3\left(a_1+d\left(\alpha_1^2(\mu-\lambda)+b_1\right)\right)\right)\\
&\quad -\frac{2\beta_0\Delta_3\left(b_2\left(2a_1 b_2 d+b_1\left(2b_2 d^2+1\right)\right)+a_2 b_1 b_2 d+a_2^2 b_1\right)}{b_2(a_2+2b_2 d)}=0,\\
\left(\frac{\phi'(\chi)}{\phi(\chi)}\right) &: \alpha_1(-d)\left(2\alpha_0^2(\lambda-\mu)+a_1 d+b_1 d^2\right)\\
&\quad +\frac{\alpha_1\left(a_2 d+b_2 d^2-1\right)\left(b_1\left(-a_2 d+2b_2 d^2+1\right)+2a_1 b_2 d\right)}{b_2(a_2+2b_2 d)}=0,\\
\left(\frac{1}{\phi(\chi)}\right)^2\left(\frac{\phi'(\chi)}{\phi(\chi)}\right) &: -\frac{1}{3}\alpha_1\left(d\left(4(\lambda-\mu)\left(3\alpha_0\beta_0+\alpha_1^2\sigma\right)-3b_1\sigma\right)-3a_1\sigma\right)\\
&\quad -\frac{\alpha_1\sigma\left(b_2\left(2a_1 b_2 d+b_1\left(2b_2 d^2+1\right)\right)+a_2 b_1 b_2 d+a_2^2 b_1\right)}{b_2(a_2+2b_2 d)}=0,\\
\left(\frac{1}{\phi(\chi)}\right)^3\left(\frac{\phi'(\chi)}{\phi(\chi)}\right) &: \frac{1}{3}(-2)\alpha_1\left(3\beta_0^2 d(\lambda-\mu)-\Delta_3\left(3a_1+d\left(\alpha_1^2(\mu-\lambda)+3b_1\right)\right)\right)\\
&\quad -\frac{2\alpha_1\Delta_3\left(b_2\left(2a_1 b_2 d+b_1\left(2b_2 d^2+1\right)\right)+a_2 b_1 b_2 d+a_2^2 b_1\right)}{b_2(a_2+2b_2 d)}=0.
\end{aligned}$$

Utilizing Mathematica to resolve these nonlinear algebraic equations obtains the results given below.

Result:

$$\left\{\begin{aligned}
\alpha_0=0,\alpha_1&=\frac{\pm\sqrt{b_1}\sqrt{3}}{2\sqrt{a_2 b_2\lambda d^3-a_2 b_2 d^3\mu-2b_2\lambda d^2+2b_2 d^2\mu}},\\
\beta_0&=\frac{\pm\sqrt{3}\sqrt{b_1}\sqrt{\Delta_3}}{2\sqrt{a_2 b_2\lambda d^3-a_2 b_2 d^3\mu-2b_2\lambda d^2+2b_2 d^2\mu}},\\
a_1&=\frac{b_1\left(a_2^2 d^2-2a_2 d+b_2 d^2+1\right)}{b_2 d(a_2 d-2)}
\end{aligned}\right\} \tag{39}$$

From Equations (12), (15), (26) and (39), obtain the rational solution of Equation (1) as follows:

For β-derivative:

$$J(x,t) = \frac{\left(\pm\sqrt{b_1}\sqrt{3}\right)\left(\sqrt{\Delta_3}\vartheta_2(\chi) + \vartheta_1(\chi)\right)e^{-dx+\frac{v}{\beta}\left(\frac{1}{\Gamma(\beta)}+t\right)^{\beta}+\epsilon}}{2\sqrt{a_2b_2\lambda d^3 - a_2b_2d^3\mu - 2b_2\lambda d^2 + 2b_2d^2\mu}}, \tag{40}$$

For M-truncated derivative:

$$J(x,t) = \frac{\pm\left(\sqrt{b_1}\sqrt{3}\right)\left(\sqrt{\Delta_3}\vartheta_2(\chi) + \vartheta_1(\chi)\right)e^{-dx+\frac{v\Gamma(\beta+1)t^{\gamma}}{\gamma}+\epsilon}}{2\sqrt{a_2b_2\lambda d^3 - a_2b_2d^3\mu - 2b_2\lambda d^2 + 2b_2d^2\mu}}, \tag{41}$$

where

$$\vartheta_1(\chi) = \frac{B_1 + \chi\sigma}{B_1\chi + B_2 + \frac{\chi^2\sigma}{2}},$$

$$\vartheta_2(\chi) = \frac{1}{B_1\chi + B_2 + \frac{\chi^2\sigma}{2}}.$$

Since the Biswas–Arshed equation is a time-space fractional model, appropriate initial and boundary conditions are necessary to ensure well-posedness. In the context of optical solitons, the initial condition at $t = 0$ typically corresponds to a localized input pulse with finite amplitude. Moreover, the boundary condition is taken as follows:

$$\lim_{|x|\to\infty} J(x,t) = 0,$$

meaning that the soliton amplitude vanishes at spatial infinity. These conditions reflect the physical reality of solitary waves that are localized in space and evolve from prescribed input profiles in time.

6. Physical Behavior of Solitons

This section contained the physical characteristics of the gained solitons with M-truncated and β fractional derivative like kink, singular and periodic- singular types.

In Figure 1, the physical behavior of solution $J(x,t)$ with the M-truncated fractional derivative shown in Equation (29), in Figure 1a 3-dim, with $d = 0.1, \nu = -0.5, \delta = -1$, $\lambda = -0.2, \mu = -1.2, a_2 = 0.2, b_1 = 2, b_2 = -0.5; \xi = 0; \beta = 0.5; \tau = 0.5$, Figure 1b 2-dim with $t = 0, 1, 2, 3$ and Figure 1c contour.

In Figure 2, the physical behavior of solution $J(x,t)$ with the β fractional derivative shown in Equation (31), in Figure 2a 3-dim, with $d = 0.1, \nu = -0.5, \delta = -1, \lambda = -0.2$, $\mu = -1.2, a_2 = 0.2, b_1 = 2, b_2 = -0.5; \xi = 0; \beta = 0.5; \tau = 0.5; \alpha = 1$, Figure 2b 2-dim with $t = 0, 1, 2, 3$ and Figure 2c contour.

In Figure 3, the physical behavior of solution $J(x,t)$ with the M-truncated fractional derivative shown in Equation (34), in Figure 3a 3-dim, with $d = 0.1, \nu = -0.5, \delta = -1$, $\lambda = -0.2, \mu = -1.2, a_2 = 0.2, b_1 = 2, b_2 = -0.5; \xi = 0; \beta = 0.5; \tau = 0.5$, Figure 3b 2-dim with $t = 0, 1, 2, 3$ and Figure 3c contour.

In Figure 4, the physical behavior of solution $J(x,t)$ with the β fractional derivative shown in Equation (37), in Figure 4a 3-dim, with $d = 0.1, \nu = -0.5, \delta = -1, \lambda = -0.2$, $\mu = -1.2, a_2 = 0.2, b_1 = 2, b_2 = -0.5; \xi = 0; \beta = 0.5; \tau = 0.5; \alpha = 1$, Figure 4b 2-dim with $t = 0, 1, 2, 3$ and Figure 4c contour.

In Figure 5, the physical behavior of solution $J(x,t)$ with the M-truncated fractional derivative shown in Equation (35), in Figure 5a 3-dim, with $d = 0.1, \nu = -0.5, \delta = -1$, $\lambda = -0.2, \mu = -1.2, a_2 = 0.2, b_1 = 2, b_2 = -0.5; \xi = 0; \beta = 0.5; \tau = 0.5$, Figure 5b 2-dim with $t = 0, 1, 2, 3$ and Figure 5c contour.

In Figure 6, the physical behavior of solution $J(x,t)$ with the β fractional derivative shown in Equation (38), in Figure 6a 3-dim, with $d = 0.1, \nu = -0.5, \delta = -1, \lambda = -0.2$,

$\mu = -1.2, a_2 = 0.2, b_1 = 2, b_2 = -0.5; \xi = 0; \beta = 0.8; \tau = 0.5$, Figure 6b 2-dim with $t = 0, 1, 2, 3$ and Figure 6c contour.

In Figures 1–6 same behavior of the soliton with M-truncated and β fractional derivative.

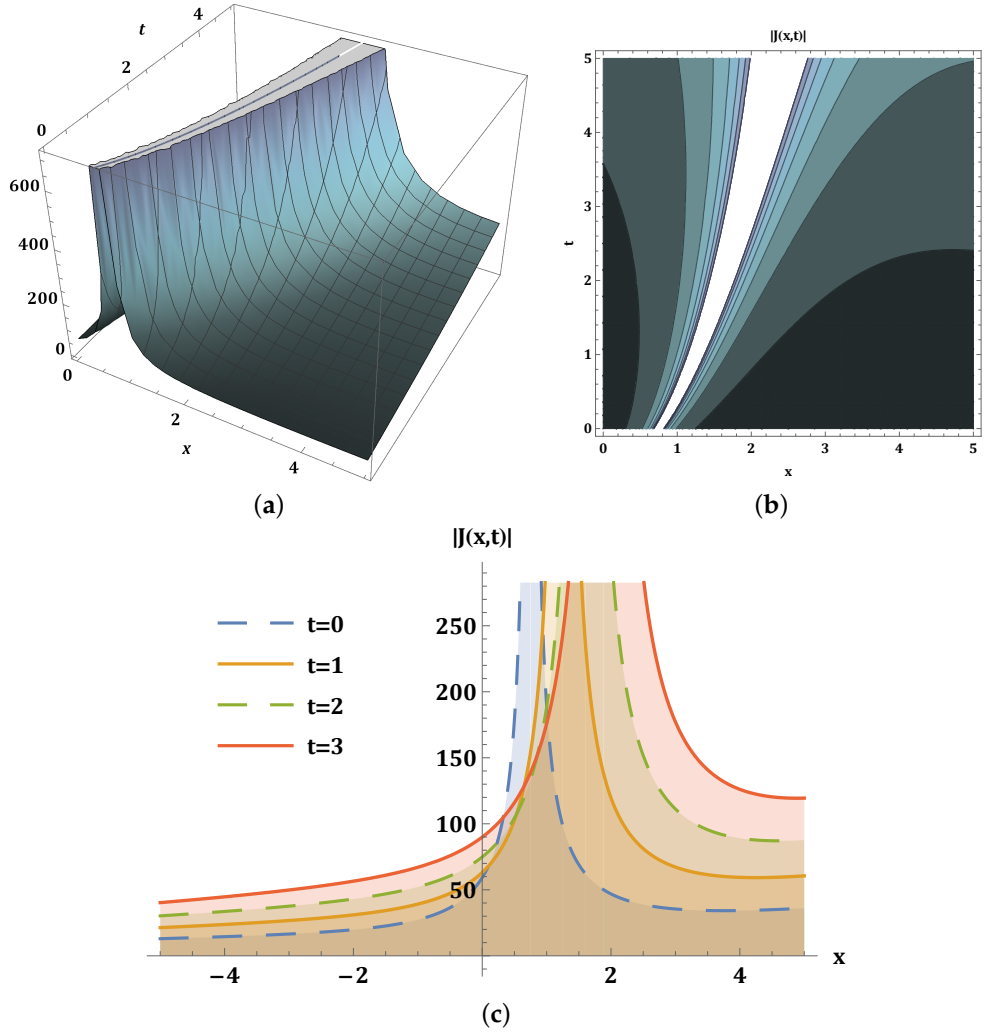

Figure 1. Physical behavior of $J(x,t)$ shown in Equation (29) in (**a**) 3-dim, (**b**) 2-dim and (**c**) contour graphs.

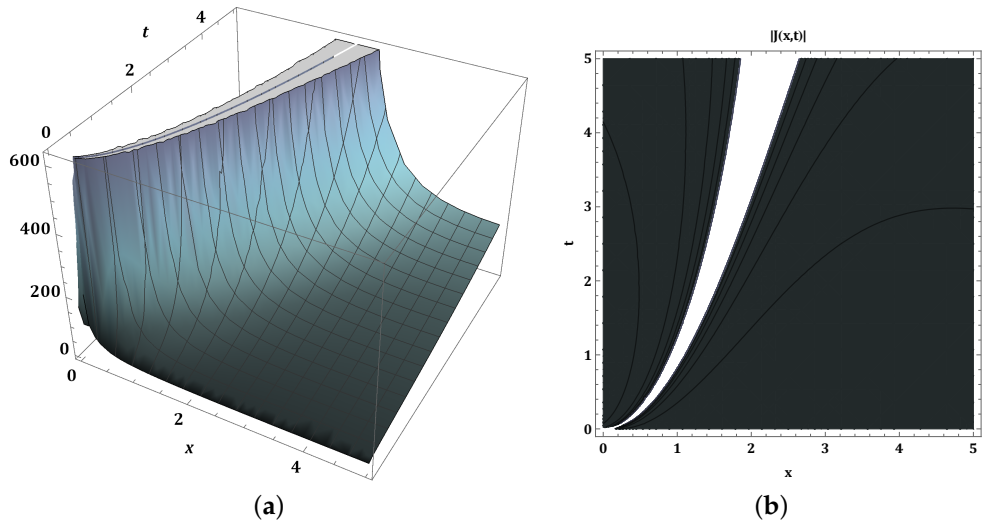

Figure 2. *Cont.*

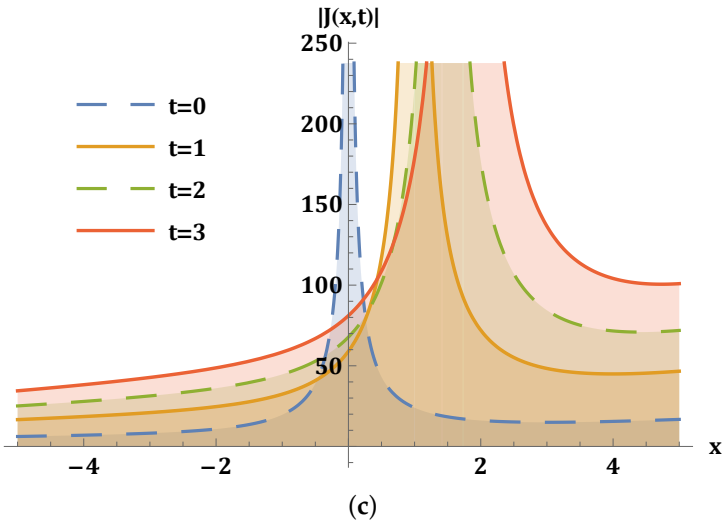

Figure 2. Physical behavior of $J(x,t)$ shown in Equation (31) in (**a**) 3-dim, (**b**) 2-dim and (**c**) contour graphs.

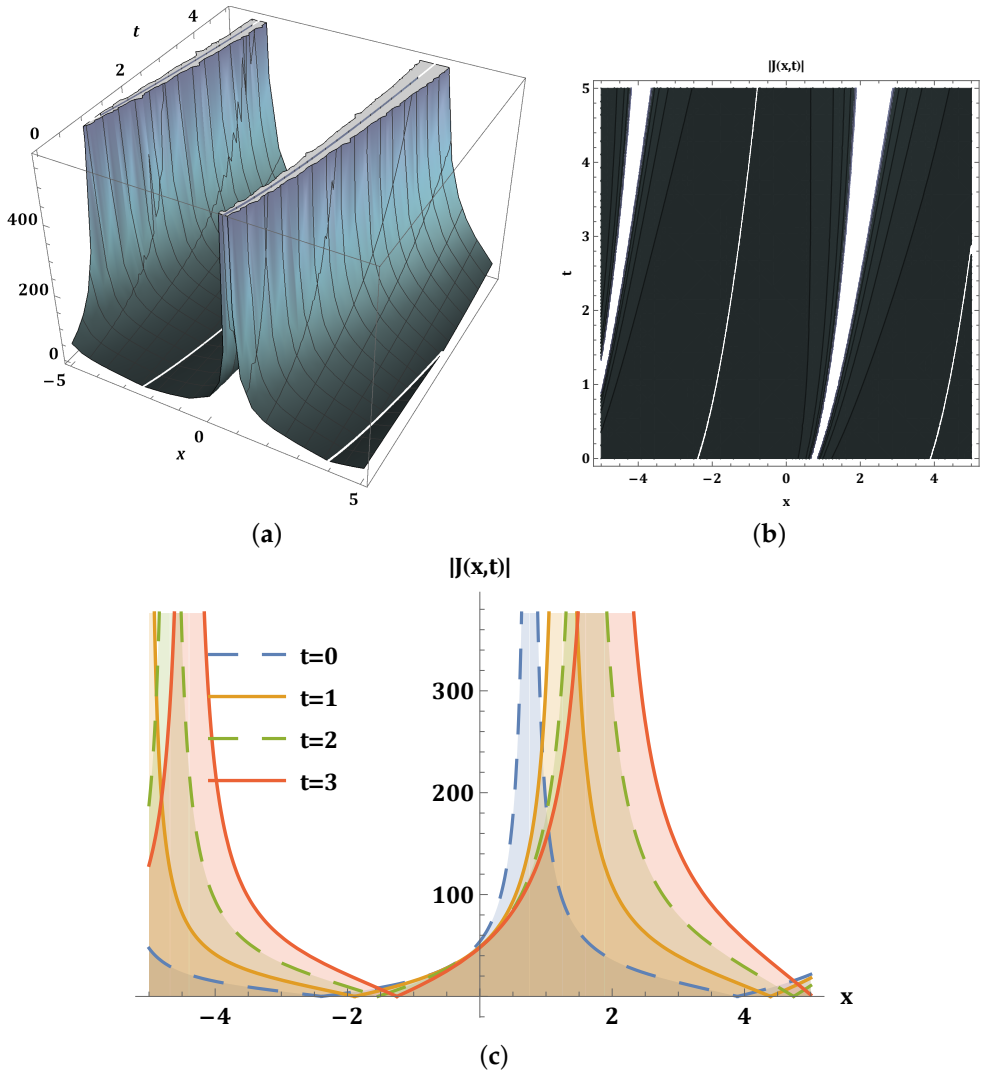

Figure 3. Physical behavior of $J(x,t)$ shown in Equation (34) in (**a**) 3-dim, (**b**) 2-dim and (**c**) contour graphs.

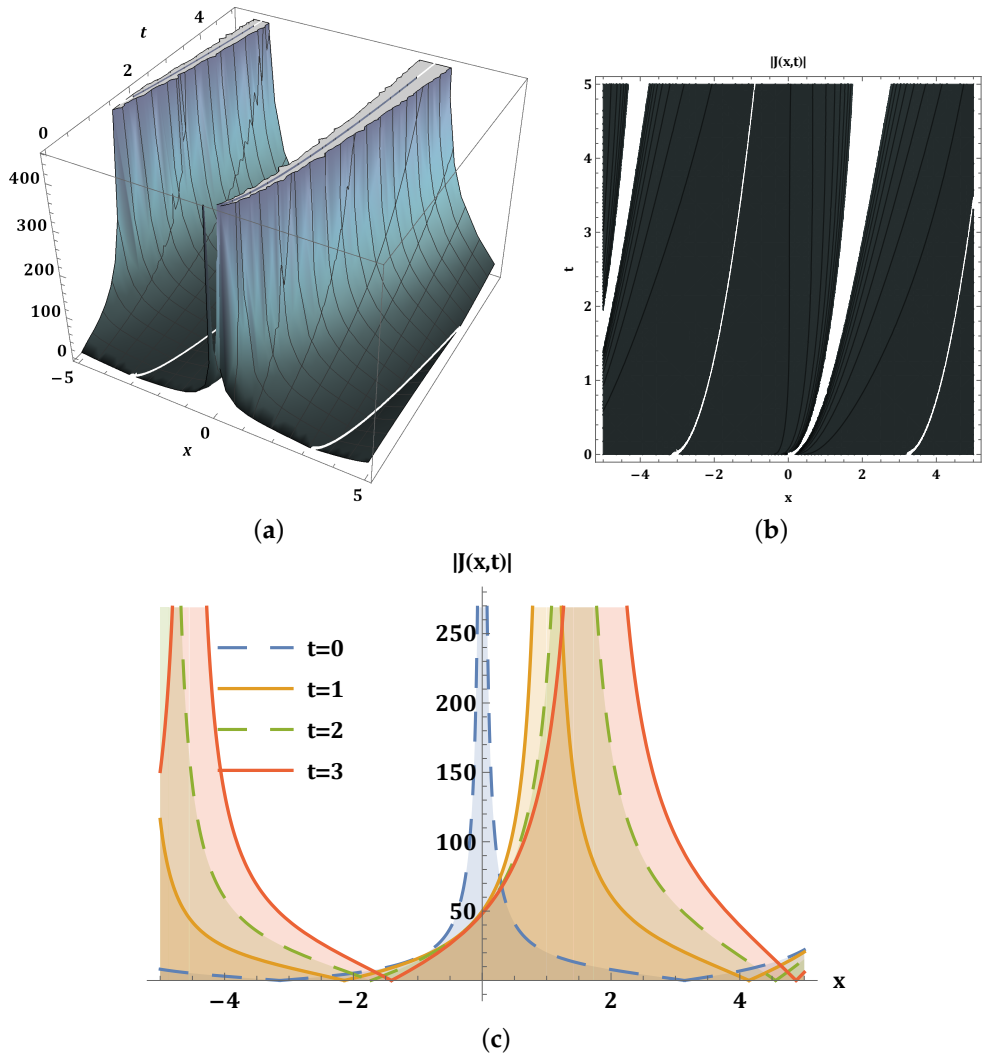

Figure 4. Physical behavior of $J(x,t)$ shown in Equation (37) in (**a**) 3-dim, (**b**) 2-dim and (**c**) contour graphs.

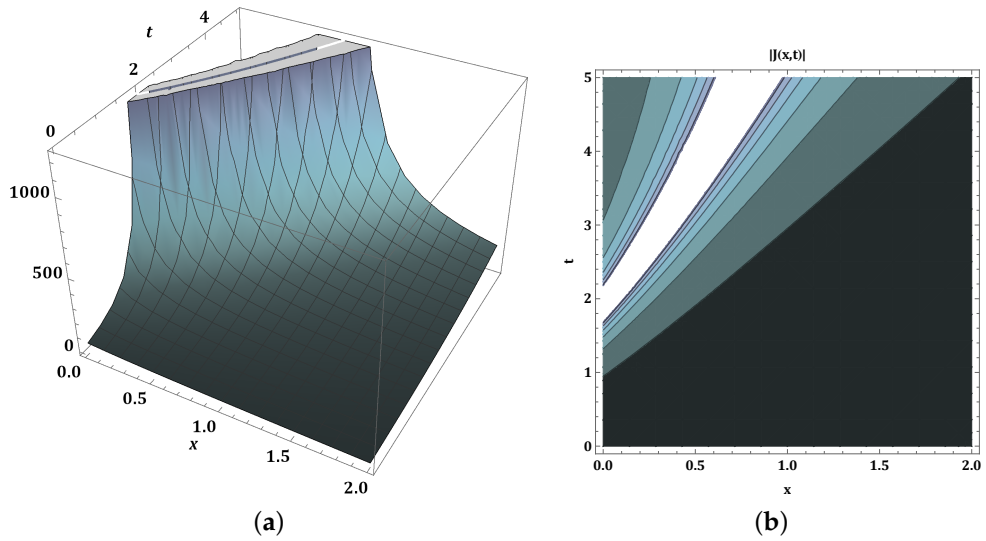

Figure 5. *Cont.*

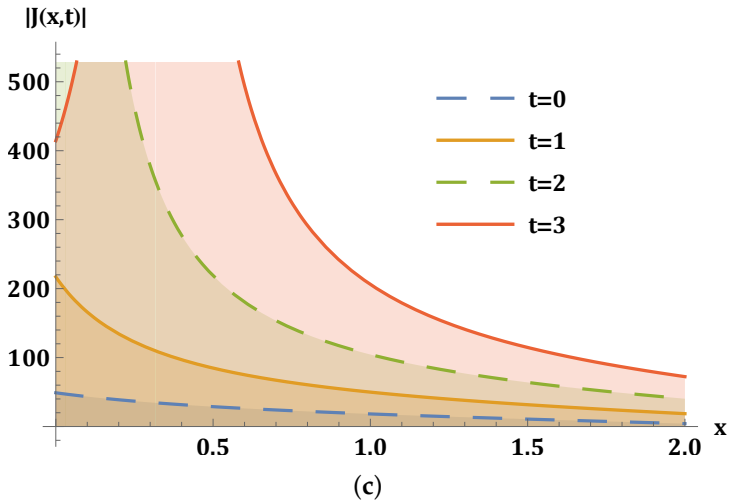

Figure 5. Physical behavior of $J(x,t)$ shown in Equation (35) in (**a**) 3-dim, (**b**) 2-dim and (**c**) contour graphs.

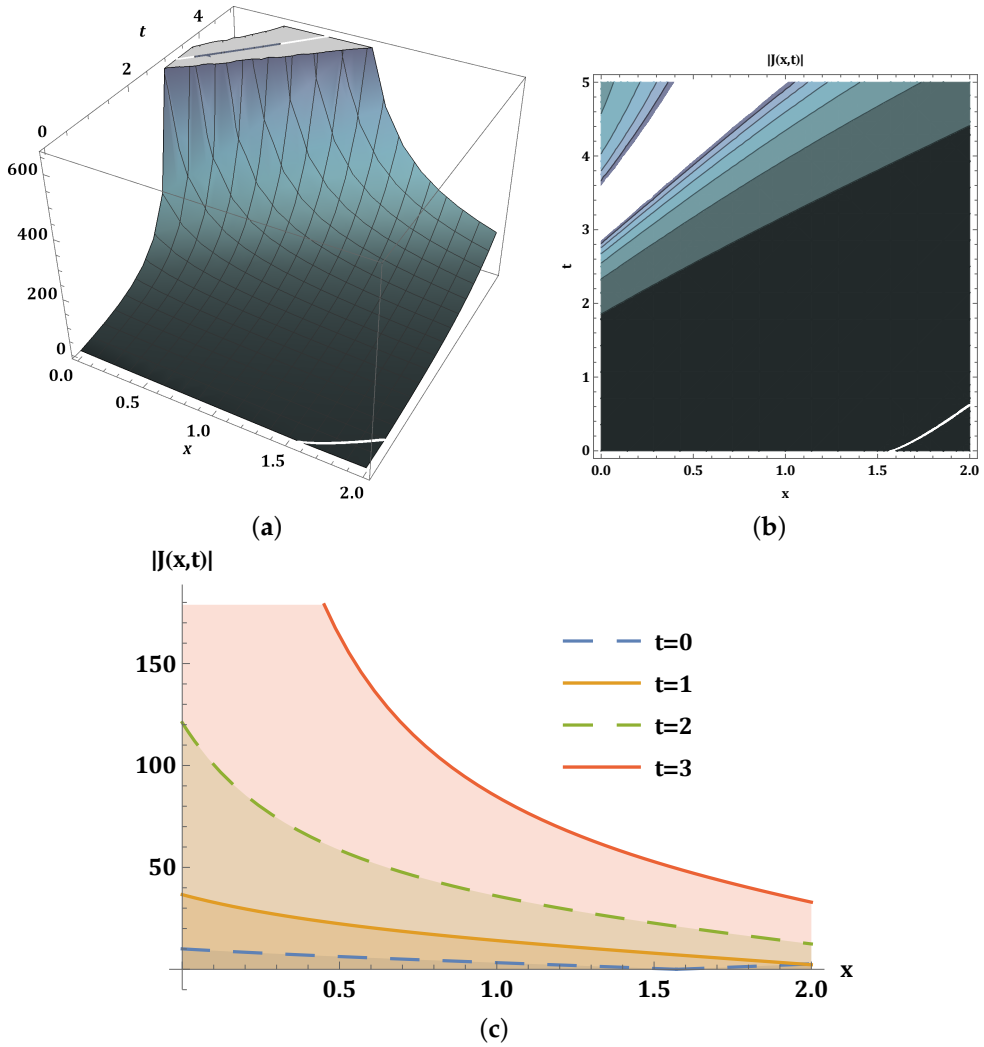

Figure 6. Physical behavior of $J(x,t)$ shown in Equation (38) in (**a**) 3-dim, (**b**) 2-dim and (**c**) contour graphs.

To highlight the influence of fractional dynamics, we performed a parametric analysis of the obtained soliton solutions with respect to the fractional orders β and γ. The results show that varying β or γ strongly affects the amplitude, width, and stability of the soliton profiles. For example, decreasing β from 0.9 to 0.5 leads to broader and slower-decaying

waveforms, reflecting enhanced memory effects. Conversely, values closer to unity recover sharper, more localized solitons resembling the classical case. A similar trend is observed for γ, where smaller values correspond to stronger fading memory and slower propagation dynamics. These findings confirm that fractional orders act as tunable parameters controlling the balance between dispersion and nonlinearity, thereby offering a richer description of wave evolution in complex media.

7. Bifurication Analysis

The bifurcation analysis of the time-fractional BA model is investigated in this section using a planar dynamical system. In order to simplify this analysis, the dynamical system in Equation (25) is assumed to be represented as follows:

$$\begin{cases} \dfrac{dP}{d\chi} = Q, \\ \dfrac{dQ}{d\chi} = -\dfrac{d_2}{d_1}P - \dfrac{d_3}{d_1}P^3, \end{cases} \tag{42}$$

where $P(\chi) = J(\chi)$ and $Q(\chi) = J^{'}(\chi)$. This system displays wave solutions of the time-fractional BA model alongside the established phase portraits in the (P, Q)-plane. The Hamiltonian canonical equations $P'(\chi) = \frac{\partial H}{\partial Q}$ and $Q'(\chi) = -\frac{\partial H}{\partial P}$ are applied to the equivalent Hamiltonian function, as illustrated in Equation (25) or Equation (42), to derive the correlated Hamiltonian function.

$$H(P, Q) = \frac{d_1}{2}Q^2 + \frac{d_2}{2}P^2 + \frac{d_3}{4}P^4. \tag{43}$$

To assess the stability of the solution, H must remain constant along trajectories ($dH/d\chi = 0$). The system (42) contains two equilibrium points (EPs): $EP_1 = (0, 0)$ and $EP_2 = (\pm\sqrt{-\frac{d_2}{d_3}}, 0)$, dependent upon the condition $\frac{d_2}{d_3} < 0$. Here, EP_2 functions as both a saddle point and a center, whereas EP_1 serves as a center point, exhibiting a trajectory as illustrated in the Figure 7. We can write the characteristic equation of the Jacobian matrix as follows:

$$\eta^2 = -(\frac{d_2}{d_1} + 3\frac{d_3}{d_1}P^2). \tag{44}$$

The characteristic roots of the EP_1 are $\pm\sqrt{E}$, where $E = -\frac{d_2}{d_1}$ and $d_1 \neq 0$, in order to assure its stability. If $E > 0$, the eigenvalues are real and of the opposite sign, implying that the specified EP_1 is a saddle point. The EP_1 is a stable center or of elliptic type if $E < 0$ and the eigenvalues are imaginary. Alternatively, the characteristic roots are $\pm i\sqrt{2E}$ for the stability of the point $(\pm\sqrt{-\frac{d_2}{d_3}}, 0)$, where $\frac{d_2}{d_3} < 0$. If $E > 0$, the eigenvalues are imaginary, signifying that the given EP_2 is a stable center. If $E < 0$, the eigenvalues are real and of opposite signs, signifying that EP_2 represents a saddle point. The phase portraits in Figure 7 illustrate how the bifurcation parameter $E = \frac{d_2}{d_1}$ governs the stability of equilibrium points in the BA model. For $E > 0$, Figure 7 demonstrate that EP_1 acts as an unstable saddle point with divergent trajectories, while EP_2 functions as a stable center enclosed by periodic orbits. On the contrary, when $E < 0$, Figure 7, the stability is reversed: EP_1 converts into a stable center defined by closed orbits, while EP_2 becomes an unstable saddle. The contour plots provide additional validation for these systems, illustrating energy level curves that correspond with saddle (hyperbolic) and center (elliptic) dynamics. For the Hamiltonian system Equation (43), we produce three-dimensional representations of the total surface energy, as illustrated in Figure 8. This research highlights the model's complex dynamical structure, with implications for solitary and periodic wave phenomena.

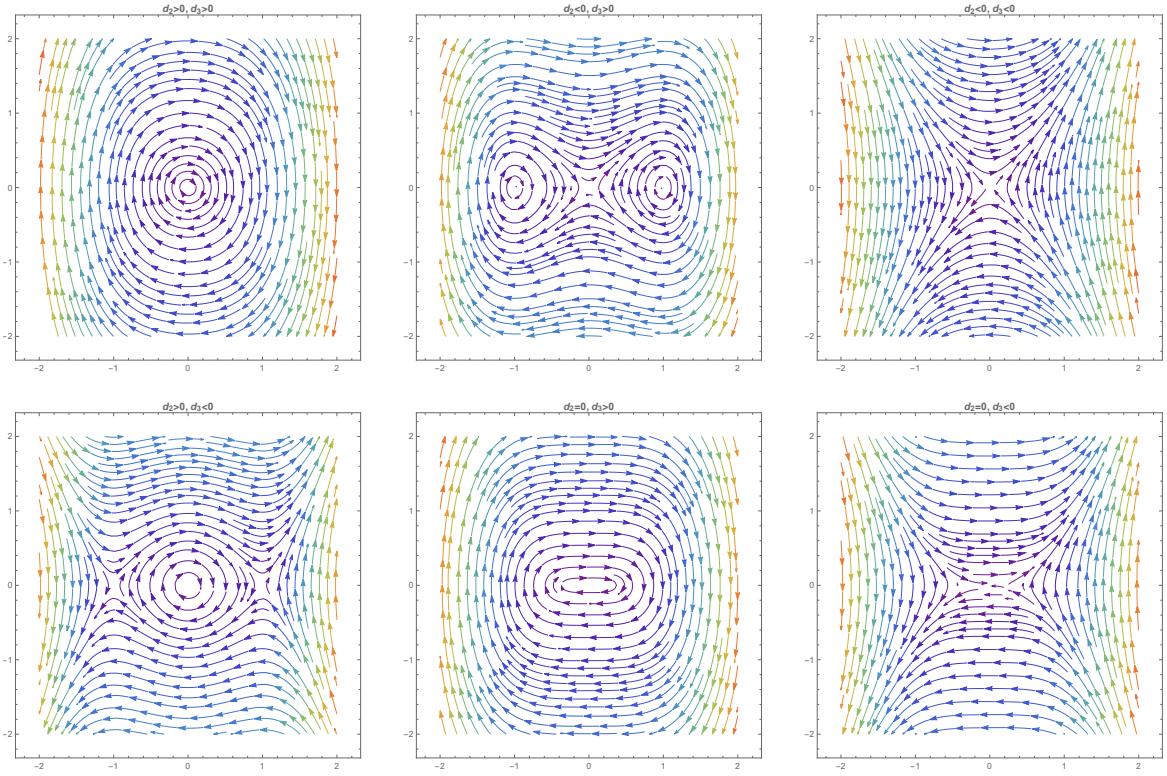

Figure 7. Phase Portrait.

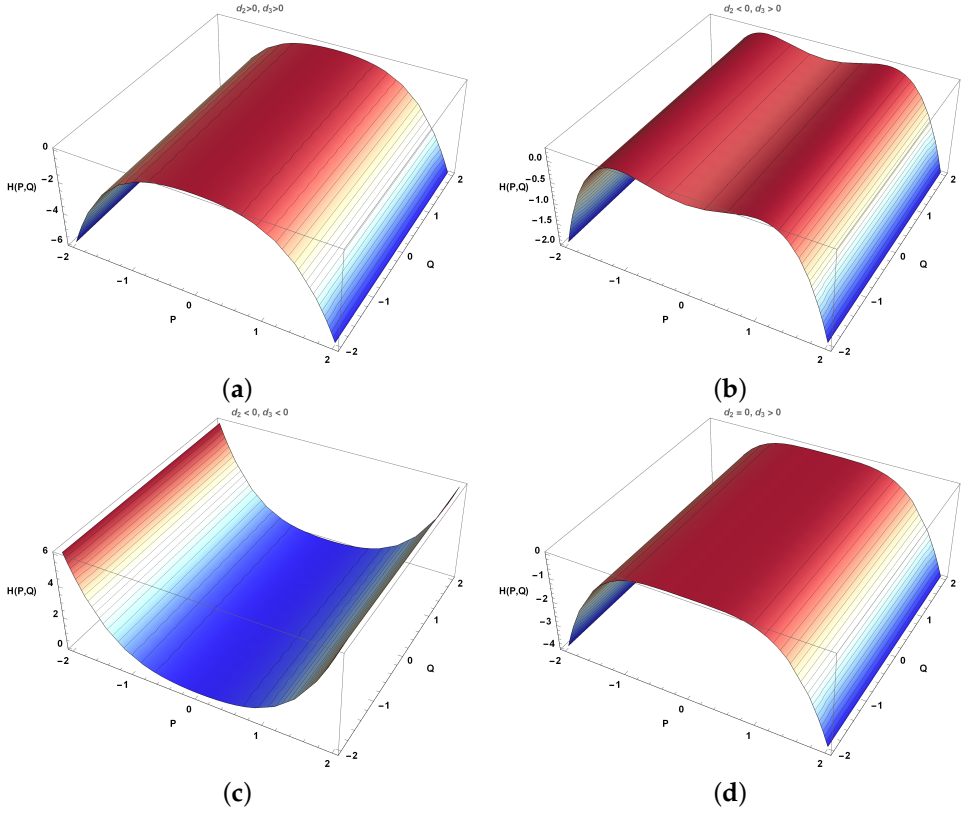

Figure 8. *Cont.*

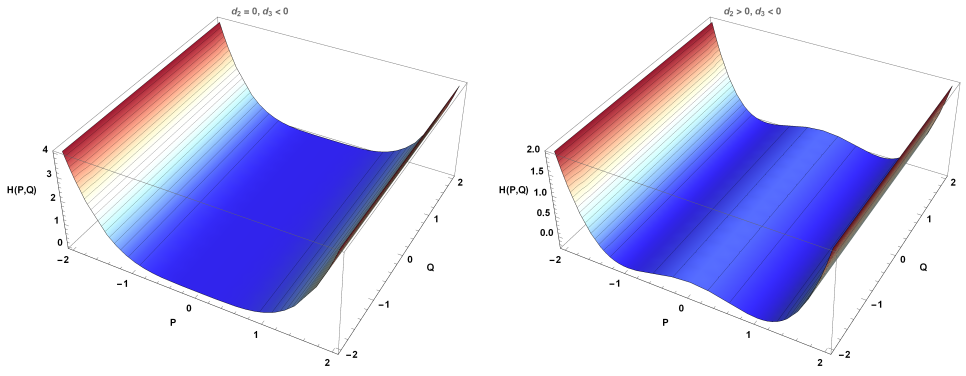

(**e**) (**f**)

Figure 8. Three-dimensional representations of the total surface energy.

8. Conclusions

This study presents new optical soliton solutions to the time-fractional Biswas–Arshed (BA) equation by employing the extended simplest equation approach in conjunction with both β-fractional and M-truncated derivatives. The effectively established a range of solution types, including kink, singular, and periodic-singular forms, by choosing random values for the free parameters by using the computational program called Mathematica. These solutions are important because they provide new ideas and instruments to address the complex problems posed by higher-order and dispersive nonlinear partial differential equations. The findings not only improve the theoretical knowledge of the investigated models, but they also have potential uses in clarifying the physical events driven by these equations. The computational method shown here is a strong and efficient mathematical instrument that provides a solid basis for investigating wave solutions in a broad spectrum of complicated nonlinear models across several spheres of nonlinear research. This paper also presents a bifurcation analysis of a nonlinear second-order differential equation by transforming it to a planar dynamical system and determining its Hamiltonian structure. The critical points were obtained analytically, and their stability was assessed using linearization and eigenvalue analysis. It was demonstrated that the nature of the equilibrium points, whether saddle or center, relies on the sign of a bifurcation parameter derived from the system's coefficients. This parameter defines the boundary between qualitatively distinct solution behaviors in the phase space. These results demonstrate the importance of bifurcation theory in anticipating structural changes in nonlinear systems. Although the present study establishes exact soliton solutions and bifurcation analysis for the fractional Biswas–Arshed equation, several limitations should be acknowledged. First, the analysis is restricted to two specific fractional operators: namely the β-derivative and the M-truncated derivative, whereas other modern definitions such as the Caputo–Fabrizio or Atangana–Baleanu operators may yield different behaviors. Second, the approach is primarily analytical and does not include full-scale numerical simulations of the governing PDE, which would be necessary to validate the robustness of the solutions under perturbations. Third, the obtained soliton solutions are derived under certain parametric constraints, which may limit their direct applicability to arbitrary parameter regimes. Finally, only whole-memory operators were considered, while short-memory formulations—known to be important in fading-memory materials—remain an open direction for future research.

Author Contributions: A.Z., W.R. and A.N.—idea, methodology, investigation, writing—review and editing. M.A.A., A.S.A.N. and A.A.—formal analysis, resources, visualization, writing—review and editing. All authors have read and agreed to the published version of the manuscript.

Funding: This work was supported by the Deanship of Scientific Research, Vice Presidency for Graduate Studies and Scientific Research, King Faisal University, Saudi Arabia [KFU253379].

Data Availability Statement: All the data generated during analyzed is available in the manuscript.

Conflicts of Interest: All authors agreed there is no conflicts of interest.

References

1. Laplace, P.S. Mémoire sur les suites. *Mém. Acad. R. Sci. Paris* **1779**, *1782*, 207–309.
2. Zaman, U.H.M.; Arefin, M.A.; Akbar, M.A.; Uddin, M.H. Comprehensive dynamic-type multi-soliton solutions to the fractional order nonlinear evolution equation in ocean engineering. *AIN Shams Eng. J.* **2024**, *15*, 102935. [CrossRef]
3. Khatun, M.A.; Arefin, M.A.; Islam, M.Z.; Akbar, M.A.; Uddin, M.H. New dynamical soliton propagation of fractional type couple modified equal-width and Boussinesq equations. *Alex. Eng. J.* **2022**, *61*, 9949–9963. [CrossRef]
4. Miller, K.S. *An Introduction to the Fractional Calculus and Fractional Differential Equations*; Academic Press: Cambridge, MA, USA, 1993.
5. Iqbal, M.A.; Miah, M.M.; Ali, H.S.; Shahen, N.H.M.; Deifalla, A. New applications of the fractional derivative to extract abundant soliton solutions of the fractional order PDEs in mathematics physics. *Partial. Differ. Equ. Appl. Math.* **2024**, *9*, 100597. [CrossRef]
6. Ahmed, N.; Rani, M.; Dragomir, S.S.; Akgul, A. New exact solutions to space-time fractional telegraph equation with conformable derivative. *Int. J. Mod. Phys. B* **2023**, *37*, 2350275. [CrossRef]
7. Avazzadeh, Z.; Nikan, O.; Machado, J.A.T. Solitary wave solutions of the generalized Rosenau-KdV-RLW equation. *Mathematics* **2020**, *8*, 1601. [CrossRef]
8. Asjad, M.I.; Inç, M.; Faridi, W.A.; Bakar, M.A.; Muhammad, T.; Rezazadeh, H. Optical solitonic structures with singular and non-singular kernel for nonlinear fractional model in quantum mechanics. *Opt. Quantum Electron.* **2023**, *55*, 1–20. [CrossRef]
9. Zaman, U.H.M.; Arefin, M.A.; Akbar, M.A.; Uddin, M.H. Analyzing numerous travelling wave behavior to the fractional-order nonlinear Phi-4 and Allen-Cahn equations throughout a novel technique. *Results Phys.* **2022**, *37*, 105486. [CrossRef]
10. Sadiya, U.; Inç, M.; Arefin, M.A.; Uddin, M.H. Consistent travelling waves solutions to the non-linear time fractional Klein-Gordon and Sine-Gordon equations through extended tanh-function approach. *J. Taibah Univ. Sci.* **2022**, *16*, 594–607. [CrossRef]
11. Zaman, U.H.M.; Arefin, M.A.; Akbar, M.A.; Uddin, M.H. Analytical behavior of soliton solutions to the couple type fractional-order nonlinear evolution equations utilizing a novel technique. *Alex. Eng. J.* **2022**, *61*, 11947–11958. [CrossRef]
12. Arefin, M.A.; Khatun, M.A.; Uddin, M.H.; Inç, M. Investigation of adequate closed form travelling wave solution to the space-time fractional non-linear evolution equations. *J. Ocean Eng. Sci.* **2022**, *7*, 292–303. [CrossRef]
13. Rashed, A.S.; Mostafa, A.N.M.; Wazwaz, A.M.; Mabrouk, S.M. Dynamical behavior and soliton solutions of the Jumarie's space-time fractional modified Benjamin-Bona-Mahony equation in plasma physics. *Rom. Rep. Phys.* **2023**, *75*, 104.
14. Gasimov, Y.; Manafian, J.; Aliyeva, A. New approach of (G'/G)-expansion method to solve the fractional differential equations arising in fluid mechanics. *J. Contemp. Appl. Math.* **2025**, *15*, 124–141.
15. Mohammed, W.W.; Khatun, M.M.; Algolam, M.S.; Sidaoui, R.; Akbar, M.A. Analytical Solitary Wave Solutions of Fractional Tzitzéica Equation Using Expansion Approach: Theoretical Insights and Applications. *Fractal Fract.* **2025**, *9*, 438. [CrossRef]
16. Akbar, M.A.; Akinyemi, L.; Yao, S.W.; Jhangeer, A.; Rezazadeh, H.; Khater, M.M.; Inc, M. Soliton solutions to the Boussinesq equation through sine-Gordon method and Kudryashov method. *Results Phys.* **2021**, *25*, 104228. [CrossRef]
17. Mumtaz, A.; Shakeel, M.; Manan, A.; Shah, N.A.; Ahmed, S.F. A comparative study of new traveling wave solutions for the (2+1)-dimensional fractional Wazwaz–Kaur Boussinesq equation using novel modified (G'/G^2)-expansion method. *AIP Adv.* **2025**, *15*, 035204. [CrossRef]
18. Samir, I.; Ahmed, H.M. Retrieval of solitons and other wave solutions for stochastic nonlinear Schrödinger equation with non-local nonlinearity using the improved modified extended tanh-function method. *J. Opt.* **2024**, 1–10. [CrossRef]
19. Muniyappan, A.; Manik, K.; Saparbekova, A.; Serikbayev, N. Exploring the dynamics of dark and singular solitons in optical fibers using extended rational sinh–cosh and sine–cosine methods. *Symmetry* **2024**, *16*, 561. [CrossRef]
20. Bilal, M.; Khan, A.; Ullah, I.; Khan, H.; Alzabut, J.; Alkhawar, H.M. Application of modified extended direct algebraic method to nonlinear fractional diffusion reaction equation with cubic nonlinearity. *Boundary Value Probl.* **2025**, *2025*, 16. [CrossRef]
21. Hassaballa, A.A.; Satty, A.; Salih, M.; Adam, A.M.; MA, O.; Hamed, Z.; Mohammed, M.S.; Mahmoud, A.F.; Gumma, E.A. Analytical solutions for the nonlinear fractional stochastic KdV equation: Application of the generalized Riccati equation mapping method. *J. Appl. Sci. Eng.* **2025**, *29*, 511–519.
22. Shagolshem, S.; Bira, B.; Nagaraja, K.V. Analysis of soliton wave structure for coupled Higgs equation via Lie symmetry, Paul Painlevé approach and the Unified method. *Nonlinear Dyn.* **2025**, *113*, 11999–12020. [CrossRef]
23. Deresse, A.T.; Mussa, Y.O.; Gizaw, A.K. Approximate analytical solution of two-dimensional nonlinear time-fractional damped wave equation in the Caputo fractional derivative operator. *Math. Probl. Eng.* **2022**, *2022*, 7004412. [CrossRef]

24. Alam, M.N.; Ilhan, O.A.; Manafian, J.; Asjad, M.I.; Rezazadeh, H.; Baskonus, H.M.; Macias-Diaz, J.E. New results of some of the conformable models arising in dynamical systems. *Adv. Math. Phys.* **2022**, *2022*, 7753879. [CrossRef]
25. Abdulla, S.O.; Abdulazeez, S.T.; Modanli, M. Comparison of third-order fractional partial differential equation based on the fractional operators using the explicit finite difference method. *Alex. Eng. J.* **2023**, *70*, 37–44. [CrossRef]
26. Naeem, M.; Yasmin, H.; Shah, R.; Shah, N.A.; Chung, J.D. A comparative study of fractional partial differential equations with the help of Yang transform. *Symmetry* **2023**, *15*, 146. [CrossRef]
27. Laoubi, M.; Odibat, Z.; Maayah, B. Effective optimized decomposition algorithms for solving nonlinear fractional differential equations. *J. Comput. Nonlinear Dyn.* **2023**, *18*, 021001. [CrossRef]
28. Erman, S.; Demir, A.; Ozbilge, E. Solving inverse non-linear fractional differential equations by generalized Chelyshkov wavelets. *Alex. Eng. J.* **2023**, *66*, 947–956. [CrossRef]
29. Chatzarakis, G.E.; Logaarasi, K. Forced oscillation of impulsive fractional partial differential equations. *Partial Differ. Equ. Appl. Math.* **2023**, *7*, 100478. [CrossRef]
30. Kumar, D.; Dubey, V.P.; Dubey, S.; Singh, J.; Alshehri, A.M. Computational analysis of local fractional partial differential equations in realm of fractal calculus. *Chaos Solitons Fractals* **2023**, *167*, 113009. [CrossRef]
31. Alesemi, M.; Shahrani, J.S.A.; Iqbal, N.; Shah, R.; Nonlaopon, K. Analysis and numerical simulation of system of fractional partial differential equations with non-singular kernel operators. *Symmetry* **2023**, *15*, 233. [CrossRef]
32. Alderremy, A.A.; Shah, R.; Shah, N.A.; Aly, S.; Nonlaopon, K. Comparison of two modified analytical approaches for the systems of time fractional partial differential equations. *AIMS Math.* **2023**, *8*, 7142–7162. [CrossRef]
33. Mallick, B.; Sahu, P.K.; Routaray, M. An iterative method for solving time-fractional partial differential equations with proportional delays. *Mathematics* **2023**, *11*, 74.
34. Sultana, M.; Arshad, U.; Abdel-Aty, A.H.; Akgül, A.; Mahmoud, M.; Eleuch, H. New numerical approach of solving highly nonlinear fractional partial differential equations via fractional novel analytical method. *Fractal Fract.* **2022**, *6*, 512. [CrossRef]
35. Razzaq, W.; Zafar, A.; Nazir, A.; Ahmad, H.; Zaagan, A.A. Dark, bright and singular optical solitons for Biswas–Milovic equation with Kerr and dual power law nonlinearities. *Mod. Phys. Lett. B* **2024**, *39*, 2450443. [CrossRef]
36. Mohamed, M.; Yousif, M.; Hamza, A.E. Solving nonlinear fractional partial differential equations using the Elzaki transform method and the homotopy perturbation method. *Abstr. Appl. Anal.* **2022**, *2022*, 743234. [CrossRef]
37. Rashid, S.; Ashraf, R.; Jarad, F. Strong interaction of Jafari decomposition method with nonlinear fractional-order partial differential equations arising in plasma via the singular and nonsingular kernels. *AIMS Math.* **2022**, *7*, 7936–7963. [CrossRef]
38. Alderremy, A.A.; Shah, R.; Iqbal, N.; Aly, S.; Nonlaopon, K. Fractional series solution construction for nonlinear fractional reaction-diffusion Brusselator model utilizing Laplace residual power series. *Symmetry* **2022**, *14*, 1944. [CrossRef]
39. Pandey, P.; Singh, J. An efficient computational approach for nonlinear variable order fuzzy fractional partial differential equations. *Comput. Appl. Math.* **2022**, *41*, 38. [CrossRef]
40. Biswas, A.; Arshed, S. Optical solitons in presence of higher order dispersions and absence of self-phase modulation. *Optik* **2018**, *174*, 452–459. [CrossRef]
41. Alhojilan, Y.; Ahmed, H.M.; Rabie, W.B. Stochastic solitons in birefringent fibers for Biswas–Arshed equation with multiplicative white noise via Itô calculus by modified extended mapping method. *Symmetry* **2023**, *15*, 207. [CrossRef]
42. Cinar, M.; Secer, A.; Bayram, M. On the optical soliton solutions of time-fractional Biswas–Arshed equation including the beta or M-truncated derivatives. *Opt. Quantum Electron.* **2023**, *55*, 186. [CrossRef]
43. Li, Z. Bifurcation and traveling wave solution to fractional Biswas–Arshed equation with the beta time derivative. *Chaos Solitons Fractals* **2022**, *160*, 112249. [CrossRef]
44. Akram, G.; Sadaf, M.; Zainab, I. The dynamical study of Biswas–Arshed equation via modified auxiliary equation method. *Optik* **2022**, *255*, 168614. [CrossRef]
45. Akbulut, A.; Islam, S.R. Study on the Biswas–Arshed equation with the beta time derivative. *Int. J. Appl. Comput. Math.* **2022**, *8*, 167. [CrossRef]
46. Kumar, S.; Niwas, M. New optical soliton solutions of Biswas–Arshed equation using the generalised exponential rational function approach and Kudryashov's simplest equation approach. *Pramana* **2022**, *96*, 204. [CrossRef]
47. Kudryashov, N.A. Simplest equation method to look for exact solutions of nonlinear differential equations. *Chaos Solitons Fractals* **2005**, *24*, 1217–1231. [CrossRef]
48. Kudryashov, N.A. Exact solitary waves of the Fisher equation. *Phys. Lett. A* **2005**, *342*, 99–106. [CrossRef]
49. Bilige, S.; Chaolu, T.; Wang, X. Application of the extended simplest equation method to the coupled Schrödinger–Boussinesq equation. *Appl. Math. Comput.* **2013**, *224*, 517–523. [CrossRef]
50. Bilige, S.; Chaolu, T. An extended simplest equation method and its application to several forms of the fifth-order KdV equation. *Appl. Math. Comput.* **2010**, *216*, 3146–3153. [CrossRef]
51. Shehata, M.S.; Bekir, A. New perceptions for the bright and dark soliton solutions to the modified nonlinear Schrödinger equation. *Int. J. Mod. Phys. B* **2023**, *37*, 2350204. [CrossRef]

52. Wang, K.J.; Wang, G.D. Exact traveling wave solutions for the system of the ion sound and Langmuir waves by using three effective methods. *Results Phys.* **2022**, *35*, 105390. [CrossRef]
53. Atangana, A.; Baleanu, D. New fractional derivatives with nonlocal and non-singular kernel: Theory and application to heat transfer model. *arXiv* **2016**, arXiv:1602.03408. [CrossRef]
54. Yépez-Martínez, H.; Gómez-Aguilar, J.F.; Baleanu, D. Beta-derivative and sub-equation method applied to the optical solitons in medium with parabolic law nonlinearity and higher order dispersion. *Optik* **2018**, *155*, 357–365. [CrossRef]
55. Sousa, J.V.D.C.; de Oliveira, E.C. A new truncated *M*-fractional derivative type unifying some fractional derivative types with classical properties. *arXiv* **2017**, arXiv:1704.08187.
56. Han, T.; Li, Z.; Yuan, J. Optical solitons and single traveling wave solutions of Biswas–Arshed equation in birefringent fibers with the beta-time derivative. *AIMS Math.* **2022**, *7*, 15282–15297. [CrossRef]
57. Sumelka, W.; Łuczak, B.; Gajewski, T.; Voyiadjis, G.Z. Modelling of AAA in the framework of time-fractional damage hyperelasticity. *Int. J. Solids Struct.* **2020**, *206*, 30–42. [CrossRef]
58. Zhou, Y.; Zhang, Y. Noether symmetries for fractional generalized Birkhoffian systems in terms of classical and combined Caputo derivatives. *Acta Mech.* **2020**, *231*, 3017–3029. [CrossRef]

Disclaimer/Publisher's Note: The statements, opinions and data contained in all publications are solely those of the individual author(s) and contributor(s) and not of MDPI and/or the editor(s). MDPI and/or the editor(s) disclaim responsibility for any injury to people or property resulting from any ideas, methods, instructions or products referred to in the content.